

Spent Fuel and Waste Science and Technology SAND2017-11835PE

Factors controlling SCC Initiation and Growth: Current Research at Sandia National Labs

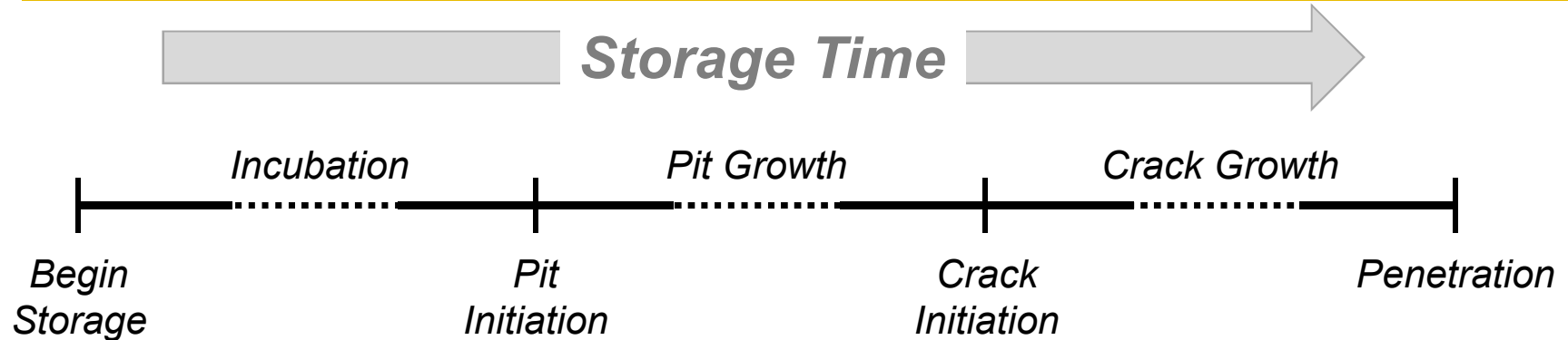
Charles Bryan
Sandia National Laboratories
Spent Fuel and Waste Science & Technology Program

ASME Subcommittee Meeting
October 30, 2017

General timeline for SCC of SNF storage canisters

- Incubation period**
- Corrosion initiation (pitting)**
- Pit growth**
- Pit-to-crack transition (crack initiation)**
- Crack growth and penetration**

Canister SCC: Important Processes



SNL — *Surface Environment, Brine Stability*

SNL/OSU — *Pitting initiation and growth,
Pit-to crack transition (experimental)*

CSM/SNL — *Pitting initiation and growth (effect of stress)*

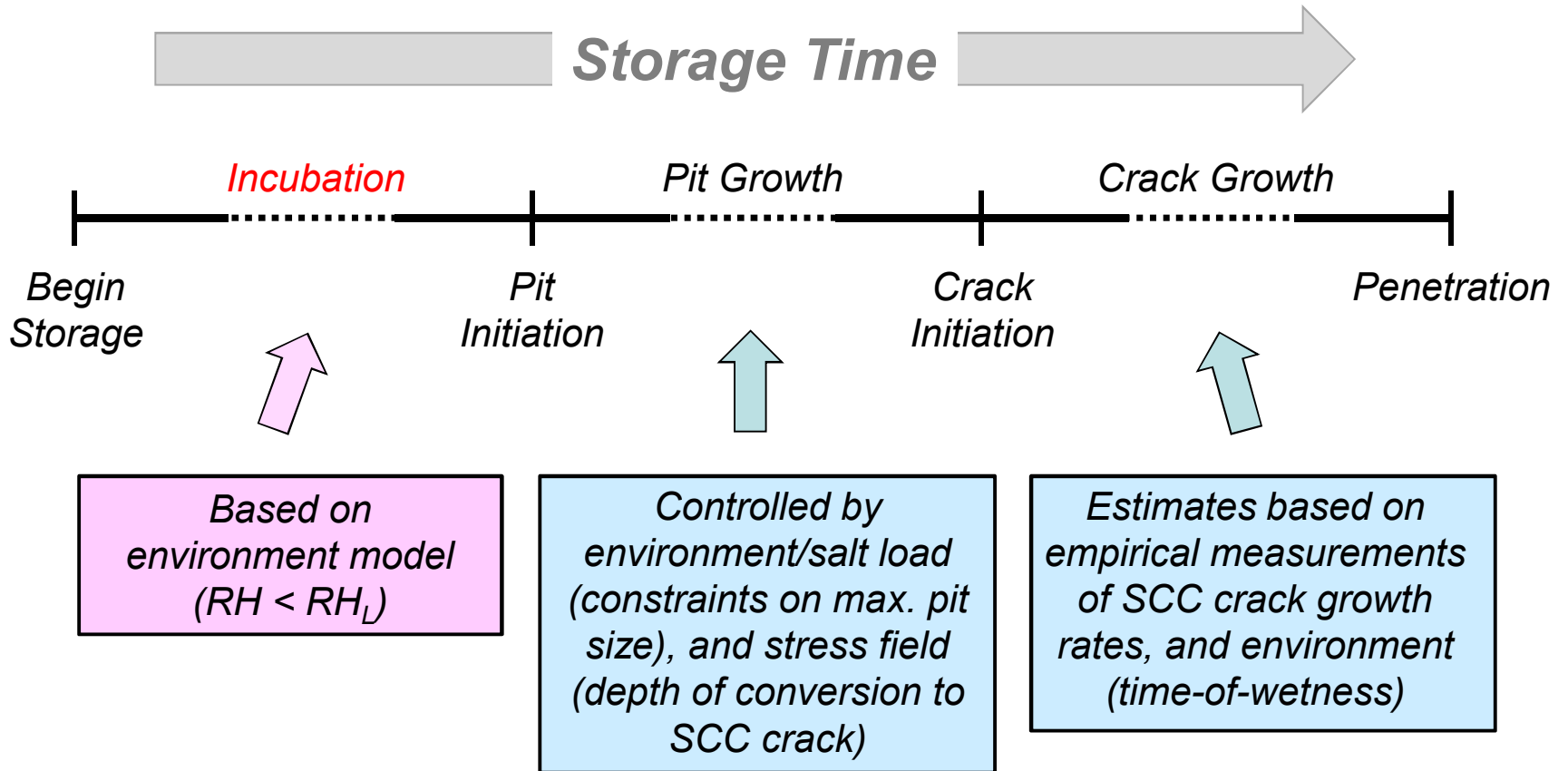
CSM — *Pit-to-Crack Transition (Modeling)*

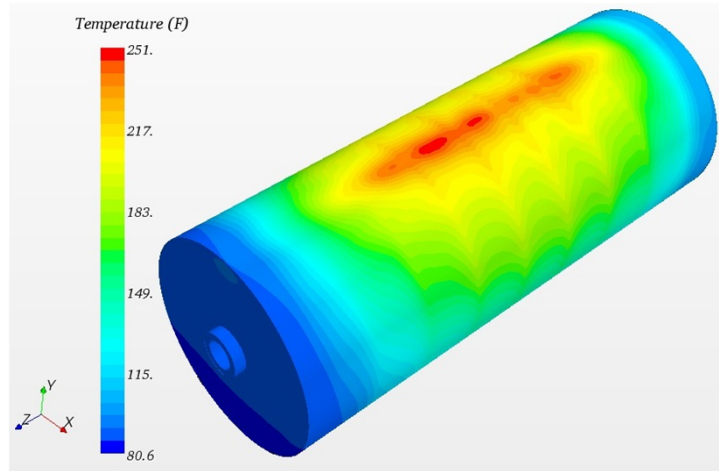
CSM/NCSU (SNL) — *SCC growth rates*

OSU (SNL) — *SCC growth rates*

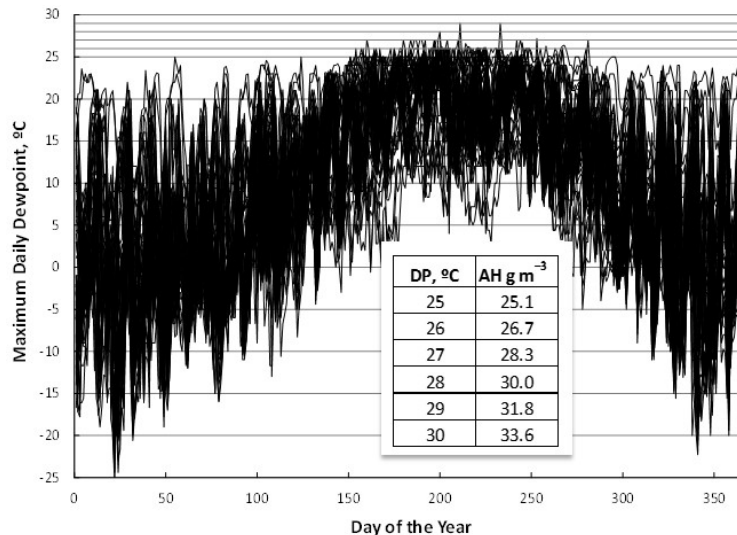
SRNL — *SCC growth rates*

Spent Fuel and Waste Science and Technology





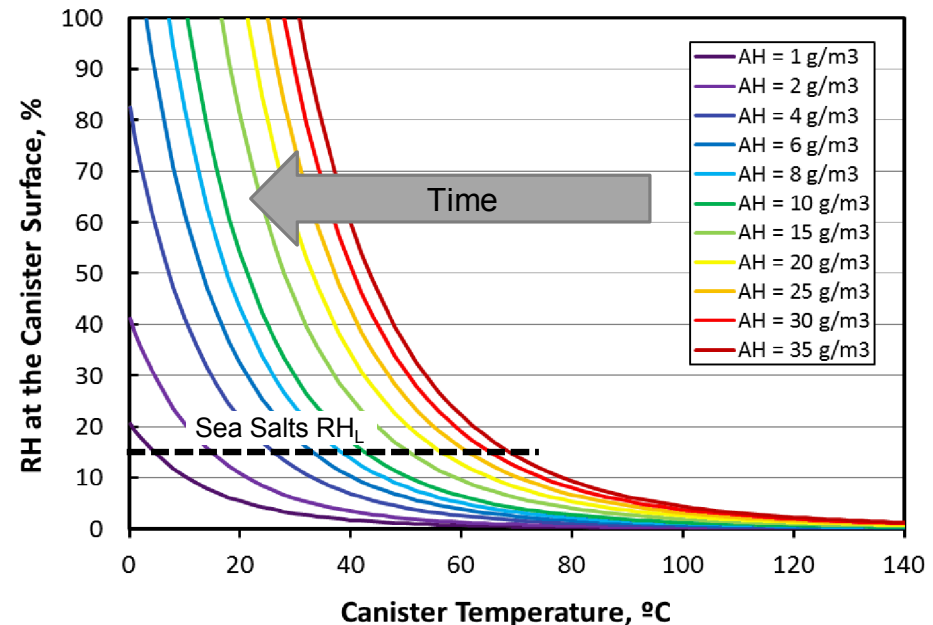
Surface temperature estimates



Site-specific National Weather Service data: daily and seasonal variations in AH

$$\text{Canister surface RH} = f(\text{Ambient AH, canister surface T})$$

Use weather data and predicted canister surface temperature to predict RH at any location and time.



Timing of corrosion initiation—point in time at which RH_L is first reached.

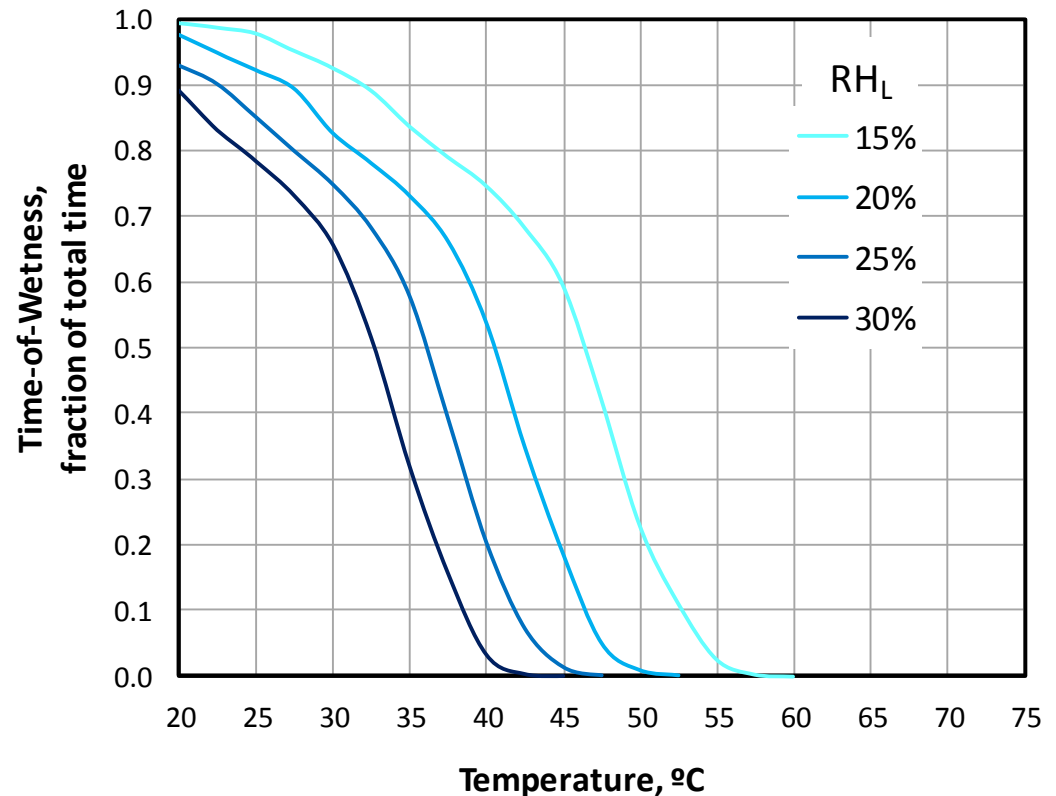
Summing time when $RH > RH_L$ provides “**time of wetness**”; time when corrosion can actually occur.

Both vary with canister surface location.

Time-of-wetness:

- Corrosion only occurs when a threshold RH (RH_L) is exceeded.
- Corrosion can start-stop on a daily or seasonal basis, as a function of changing T, AH
- Total integrated time when aqueous conditions exist is time-of-wetness
- Rationale: External cathode, required to support corrosion at the anode, is only present when aqueous conditions exist on the metal surface.
- Widely accepted approach (ASTM procedure G84-89). *However, many reasons to challenge time of wetness on a conceptual basis.* (e.g., Schindelholz et al., 2013)

Calculated time-of-wetness as a function of canister surface temperature and RH_L . Based on one year of weather data from the Oceanside Municipal Airport near the San Onofre ISFSI.



Brine composition:

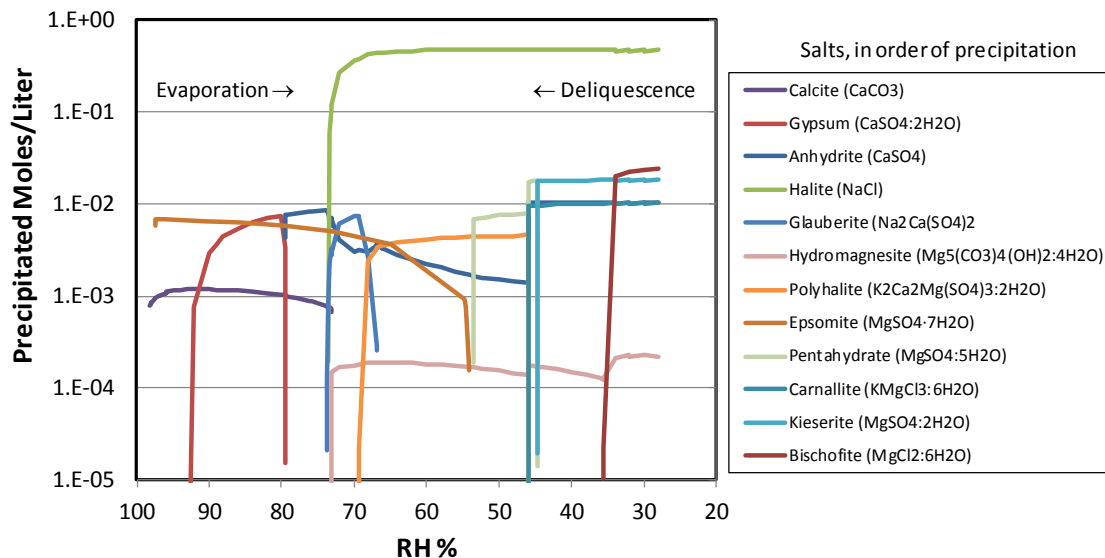
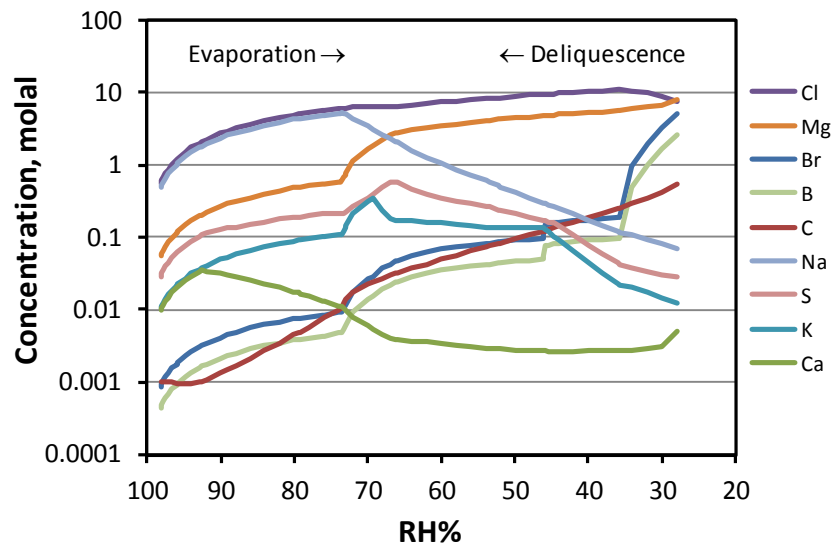
- Upon evaporation, salts precipitate and redissolve. Removed salts dictate the composition of remaining brine
- Seawater evolves towards concentrated Mg-Cl brine as NaCl precipitates
- Br and B conserved (but Pitzer database used for these calculations is not qualified for B, and may not be accurate)
- Ca, K, S are mostly removed by minerals, and are very low in the remaining brine.
- Deliquescence is the reverse of evaporation.*

Precipitated salts:

- Upon evaporation, several salts precipitate and re-dissolve.

Final assemblage determines deliquescence RH (RH_d)

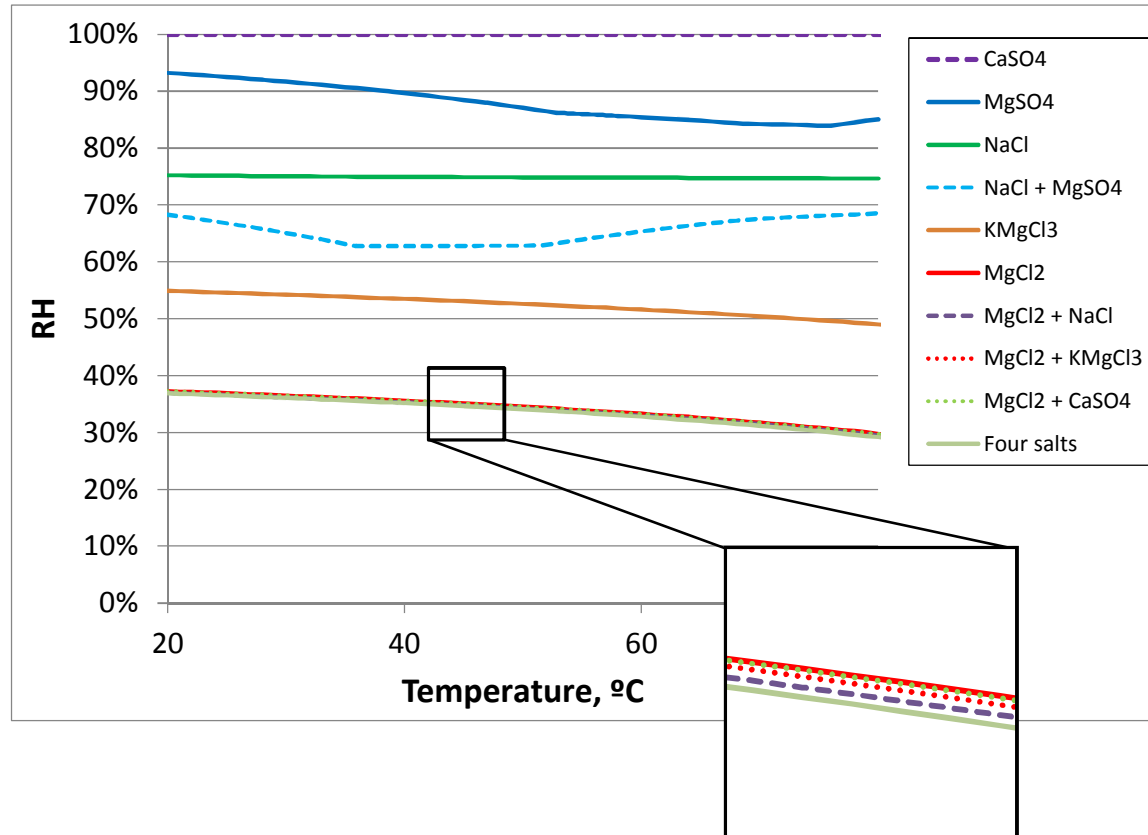
- NaCl (halite)
- $MgCl_2 \cdot 6H_2O$ (bischofite)
- $MgSO_4 \cdot 2H_2O$ (kieserite)
- $KMgCl_3 \cdot 6H_2O$ (carnallite)
- $CaSO_4$ (anhydrite)



Predicted Deliquescence of Individual Sea-Salt Minerals and of Assemblage

Deliquescence points:

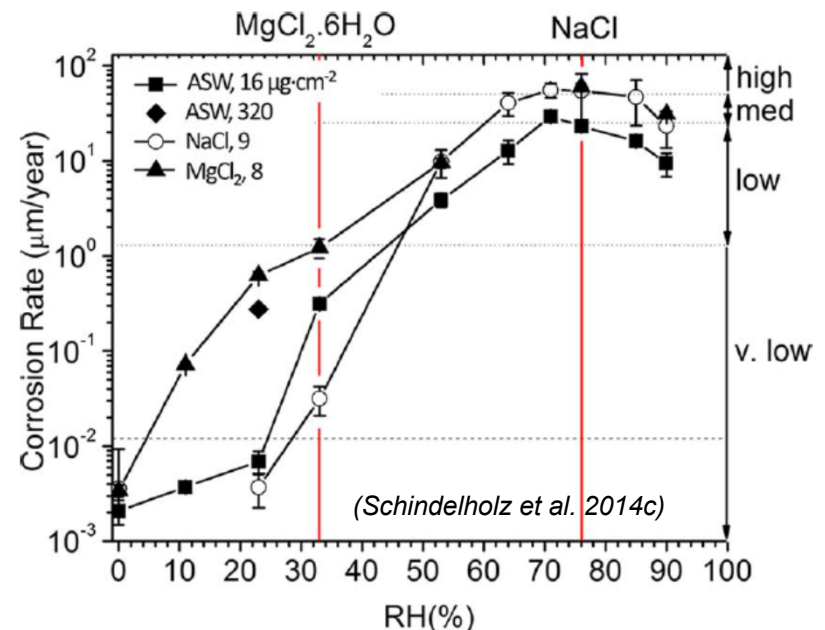
- Ca-SO_4 (gypsum or anhydrite):
DRH >99%
- Mg-SO_4 (four different hydrates):
DRH = 93-84%
- NaCl:
DRH = ~77% at all temperatures
- $\text{KMgCl}_3 \cdot 6\text{H}_2\text{O}$ (\pm sylvite):
DRH = 55-49%
- $\text{MgCl}_2 \cdot 6\text{H}_2\text{O}$:
DRH = 36-29%
- $\text{MgCl}_2 \cdot 6\text{H}_2\text{O}$ plus any or all other
salts:
DRH = ~Same as $\text{MgCl}_2 \cdot 6\text{H}_2\text{O}$



But is deliquescence $RH = RH_l$? Experimental data indicate that corrosion occurs at lower RH values...

Corrosion Below the Deliquescence RH

- **NaCl (DRH 77%)**
 - Schindelholz et al. (2014b) summarizes several studies--corrosion of mild steel at RH values of 50-58% RH. Their own study showed corrosion as low as 33% RH.
 - Once corrosion starts, it can persist to lower RH (at least 27% RH) due to highly deliquescent iron chloride salts.
- **MgCl₂ (DRH ~33%) (Schindelholz et al. 2014c)**
 - Observed corrosion (mild steel) as low as 11% RH (21°C), at a loading of 8 μg/cm².
- **Sea-salts (Schindelholz et al. 2014c)**
 - Corrosion (mild steel) observed as low as 33% RH (21°C), at a loading of 16 μg/cm².
 - Corrosion observed as low as 23% RH (21°C), at a loading of 160 mg/m².
 - Inferred that at higher sea-salts loadings, results would match MgCl₂
- **Observations of SCC**
 - NRC (2014)—**SCC** (304SS) observed as between 20% and 30% RH (variable temperatures), using sea-salts.
 - Shirai et al. (2011)—**SCC** (304SS) observed at 15% RH and 80°C, using sea-salts.
 - Fairweather et al. (2008)—**SCC** (304SS) observed at 15% RH and 45°C and 60°C, using MgCl₂.

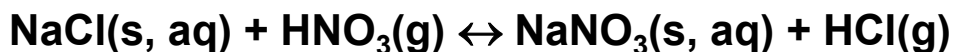


Sea-salt RH_L for SCC of 304 SS poorly constrained, and may be a function of salt load. Could be as low at 15%.

However, those experimental results assume that sea-salts are unmodified by reactions with atmospheric gases

■ Equilibrium modeling fails to consider

- Effects of atmospheric exchange reactions occurring prior to corrosion
—CO₂ and acid gas (H₂SO₄, HNO₃) absorption, HCl degassing:



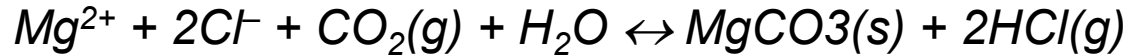
And similar reactions that occur with Ca, Mg. For instance:



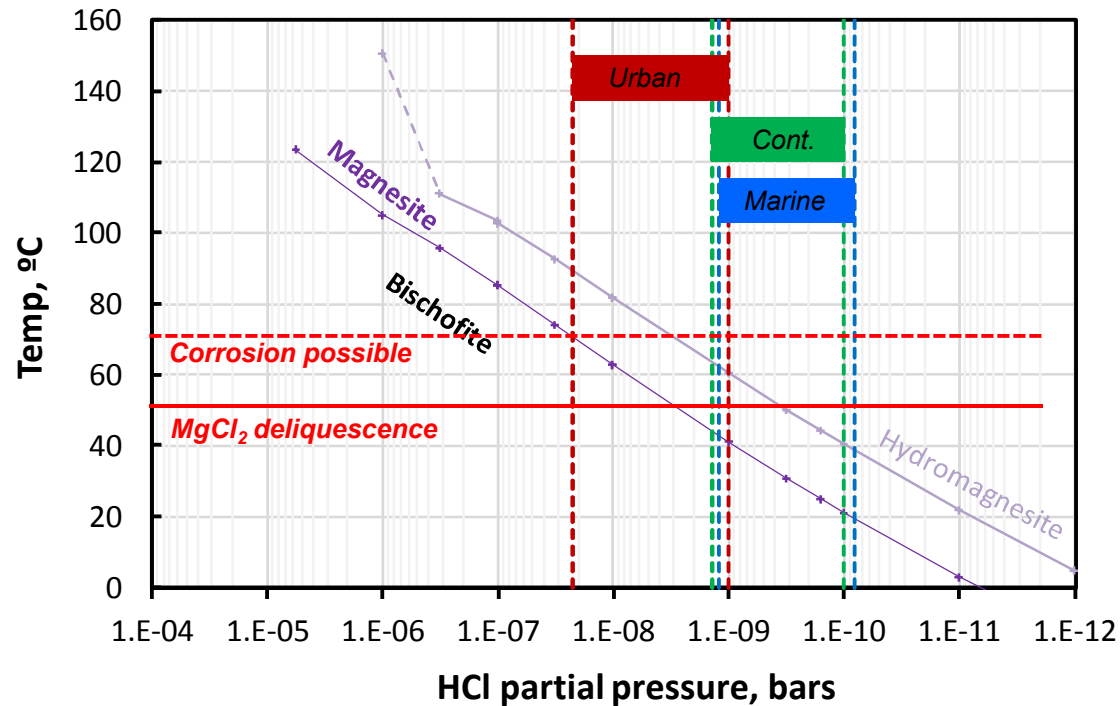
We are currently evaluating the last reaction, which is strongly temperature-dependent.

- Once corrosion initiates, effects of cathodic reactions on surface brine compositions (hydroxide generation, carbonation). We are also evaluating these reactions.

MgCl₂ Brine Stability



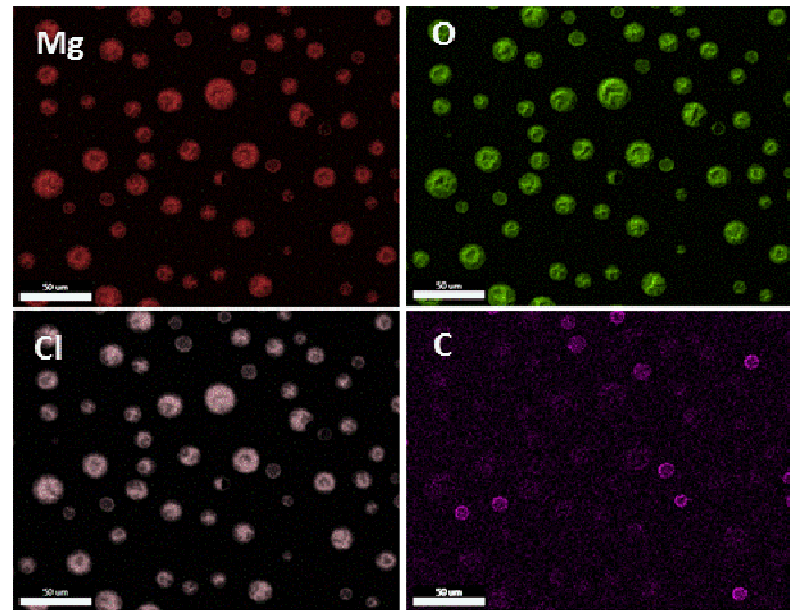
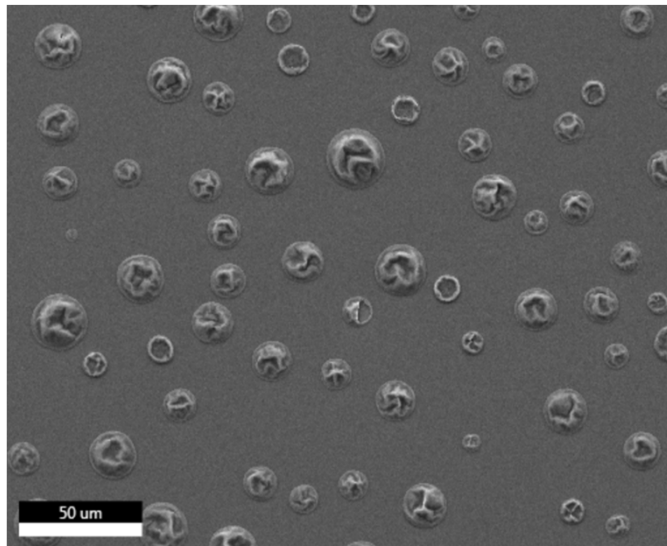
- Brines may degas, or absorb HCl, depending on background acid gas concentrations.
- MgCl₂ brine stability is a function of temperature and atmospheric HCl concentration; brine may absorb CO₂ and convert to Mg-carbonate
- MgCl₂ brine stability experiments in progress (difficult to run—air capacity for HCl is low)



Experimental results:

MgCl_2 brine at 48°C , 40%RH, $P_{\text{HCL}} = 0$

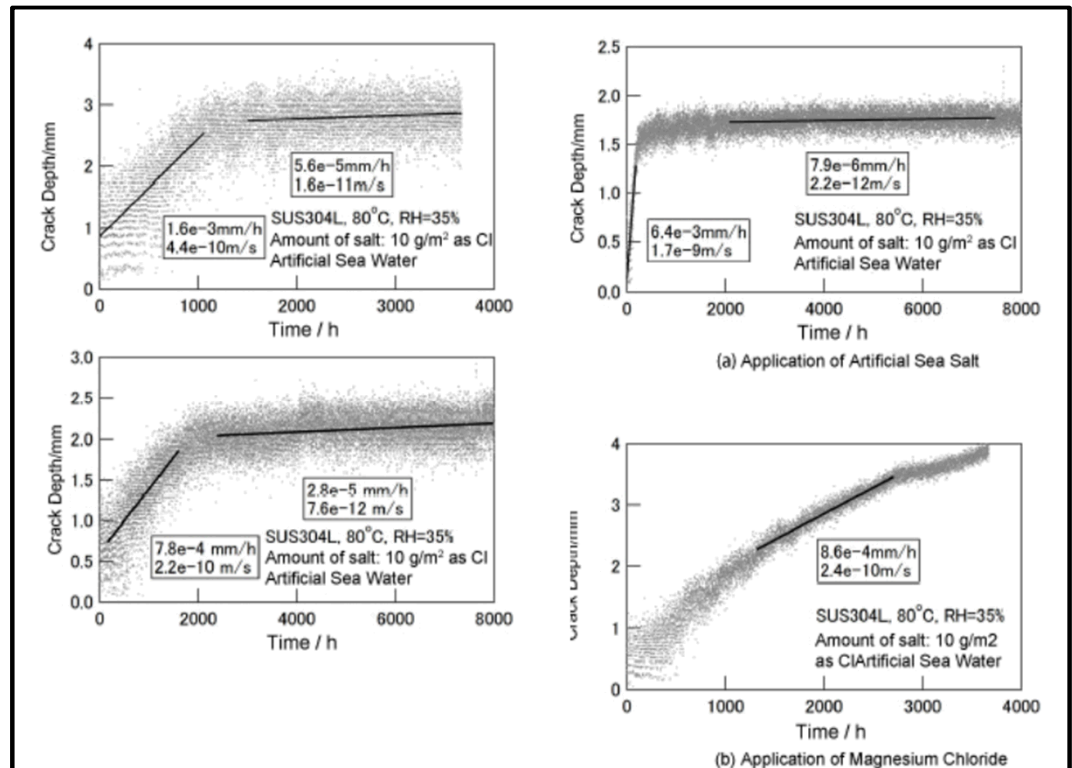
- *MgCl_2 brine, 48°C , 40% RH, for two months in an RH chamber with 2 L/minute air flow.*
- *Partial conversion to carbonate observed (some smaller droplets converted); later chemical analysis suggests 20% chloride lost. (But results erratic).*
- *Only partial conversion expected; airflow too low to support complete conversion. At 48°C , can only remove 1.3 ug (hydromagnesite) to 13 ug (magnesite) chloride per cubic meter of air.*



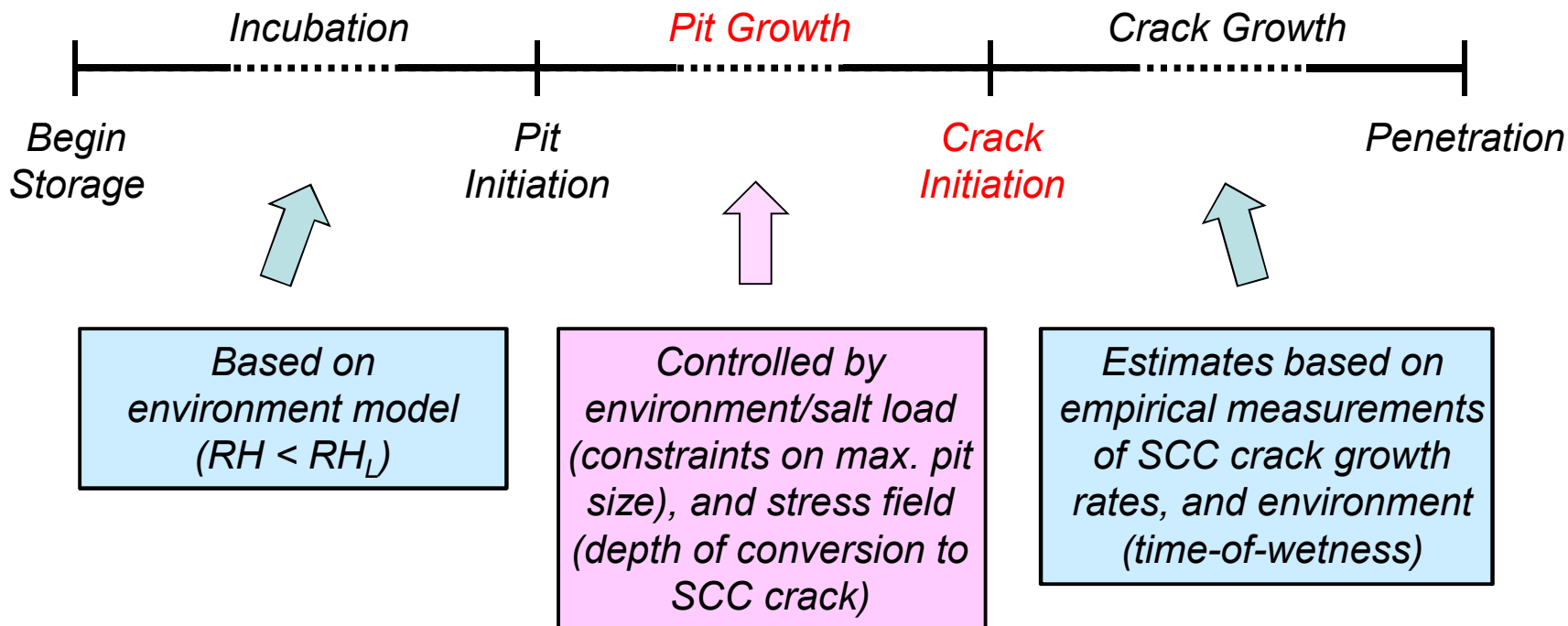
Other acid gas reactions (e.g., H₂SO₄) may be more important under field conditions. However, considering carbonation may be VERY important for interpreting laboratory experiments.

- *CRIEPI experiments: At 80°C, 35% RH, air exchange of only a cubic meter is necessary to convert the small amount of MgCl₂ present in the sea-salts to carbonate, drying out the brine.*
- *Difficulties in initiating SCC in some tests?*

We are running MgCl₂ stability experiments under identical conditions to CRIEPI right now.



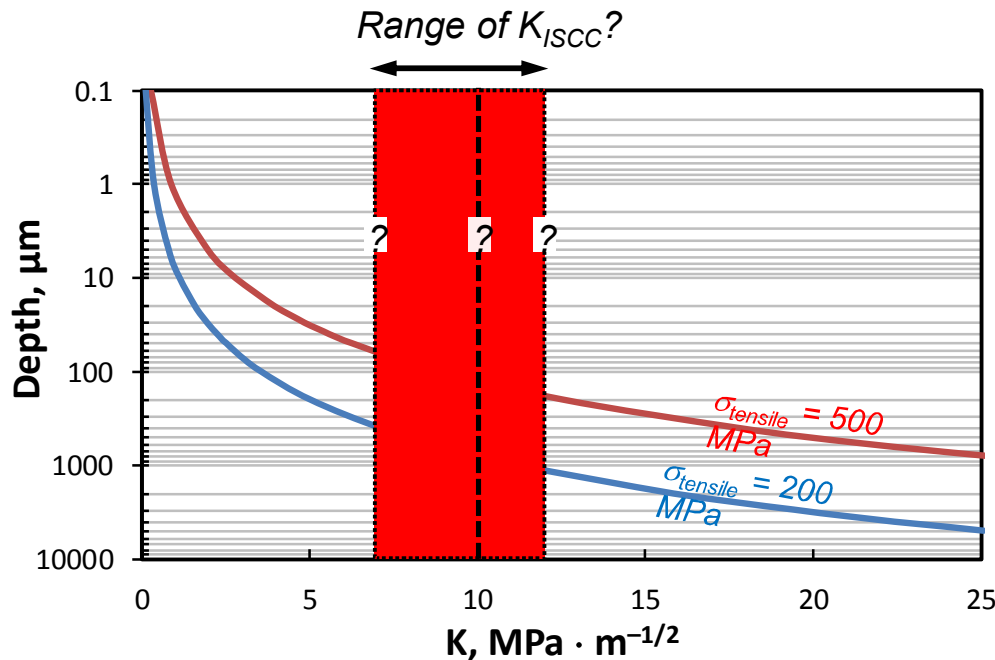
Pit Growth and SCC Crack Initiation



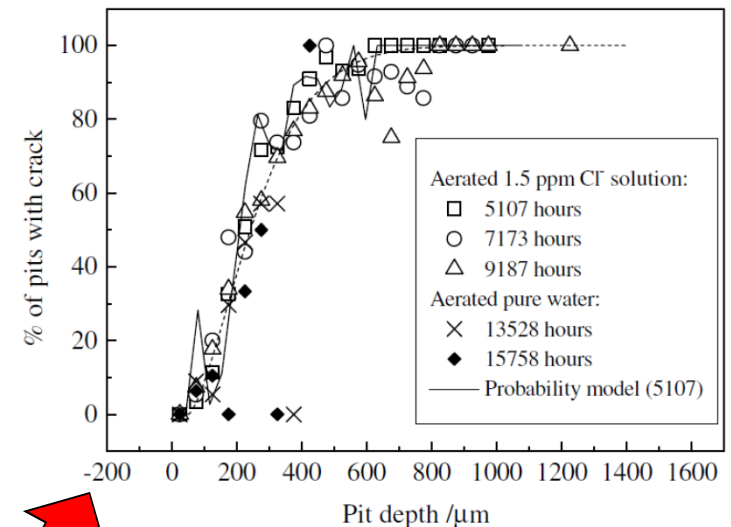
Pitting and SCC crack initiation

- Corrosion starts (pits form) once the RH_L is exceeded.
- *Pits grow over time, but for any given set of environmental conditions (T , RH , salt load), pit depths reach a limiting value.*
- Maximum pit depth model (Chen and Kelly 2010) can be used to calculate the maximum possible pit depth over time as a function of environmental parameters (temperature, RH , and deposited salt density).
- Pits generate aggressive chemistry and act as local stress focusers. SCC cracks initiate from corrosion pits on the metal surface.
- Depth of pit-to-crack transition can be *estimated* using the “Kondo criterion” (Kondo, 1985).

“Kondo criterion”. **Pit-to-crack transition** occurs when the pit depth is equal to the depth at which an equivalent-depth SCC crack would have a crack-tip stress intensity factor (K) that exceeds K_{ISCC} for the metal.



Experimental data from Turnbull et al. (2006)

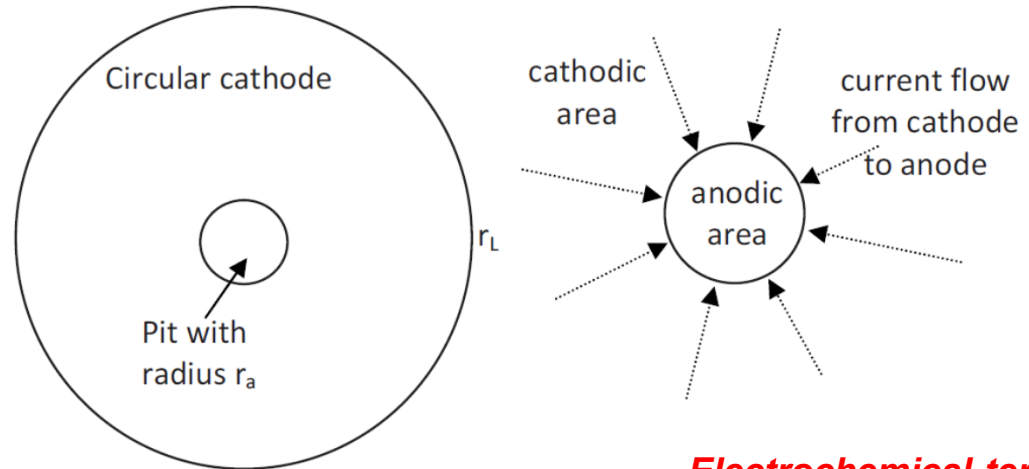


Stochastic process: As a pit deepens, the likelihood of a crack initiating increases.

Maximum Pit Size Model

Chen and Kelly (2010): Max pit size is a function of the maximum available cathode current.

Pits are modeled as being hemispherical, and stifle once the pit becomes so large that the anodic current requirement exceeds the available cathode current.



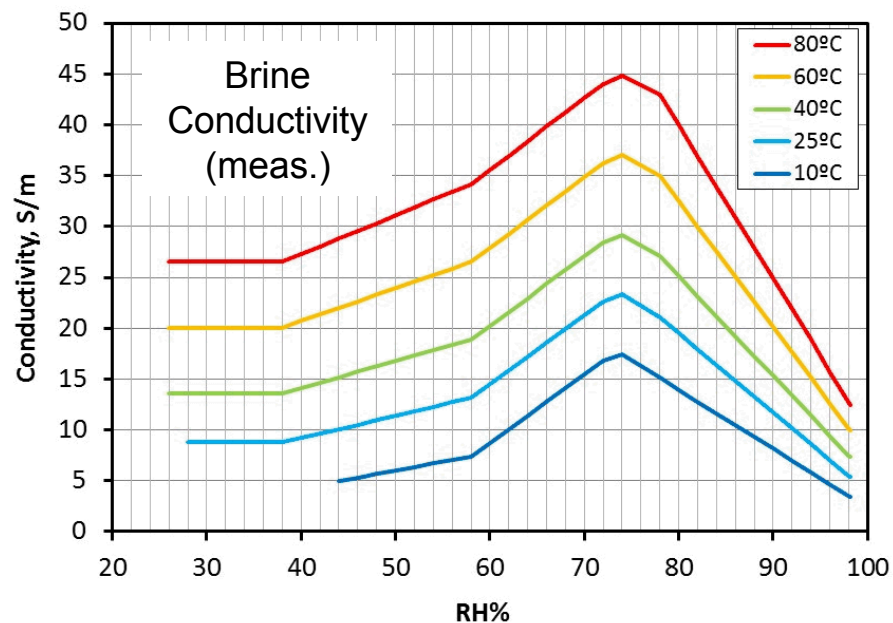
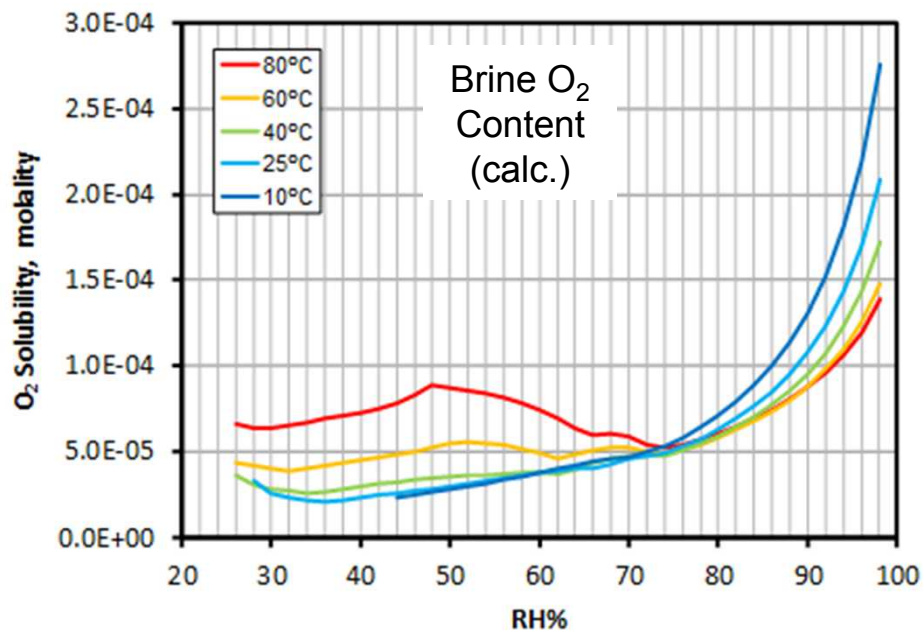
*Electrochemical term
(from cathodic
polarization curve)*

$$\ln I_{c,max} = \frac{4\pi k W_L \Delta E_{max}}{I_{c,max}} + \ln \left[\frac{\pi e r_a^2 \int_{E_{corr}}^{E_{rp}} (I_c - I_p) dE}{\Delta E_{max}} \right]$$

Labels for the equation:

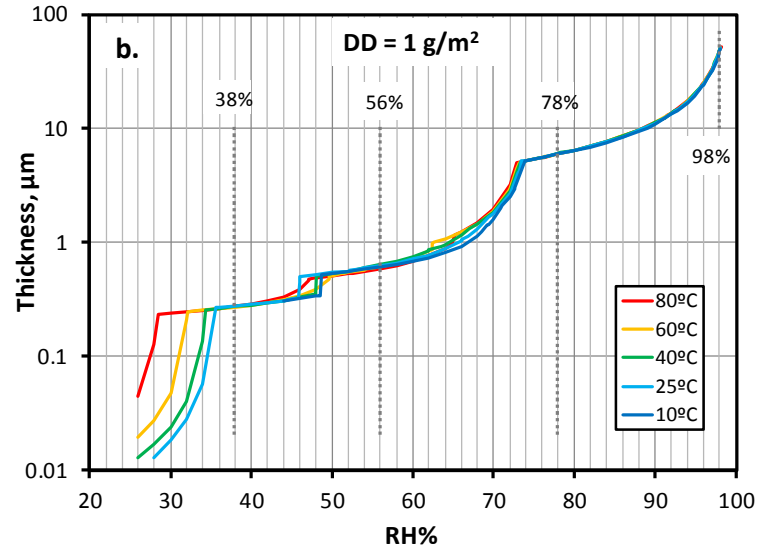
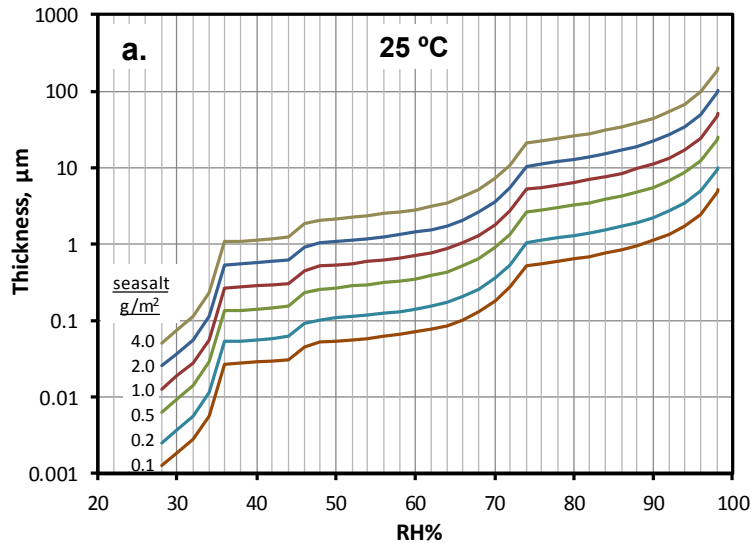
- Max. cathode current* points to $\ln I_{c,max}$
- Brine conductivity* points to k
- Brine layer thickness* points to W_L
- The entire right-hand side of the equation is circled in red.

Values are based on geochemical modeling, literature data, and measured data for brine densities and conductivities (4 brines, from 98-38% RH).



Original *Chen and Kelly* (2010) model: Based on NaCl brines (dry out at ~75% RH).

Values are based on geochemical modeling, literature data, and measured data for brine densities and conductivities (4 brines, from 98-38% RH).



Original *Chen and Kelly* (2010) model:
Based on NaCl brines
(dry out at ~75% RH).

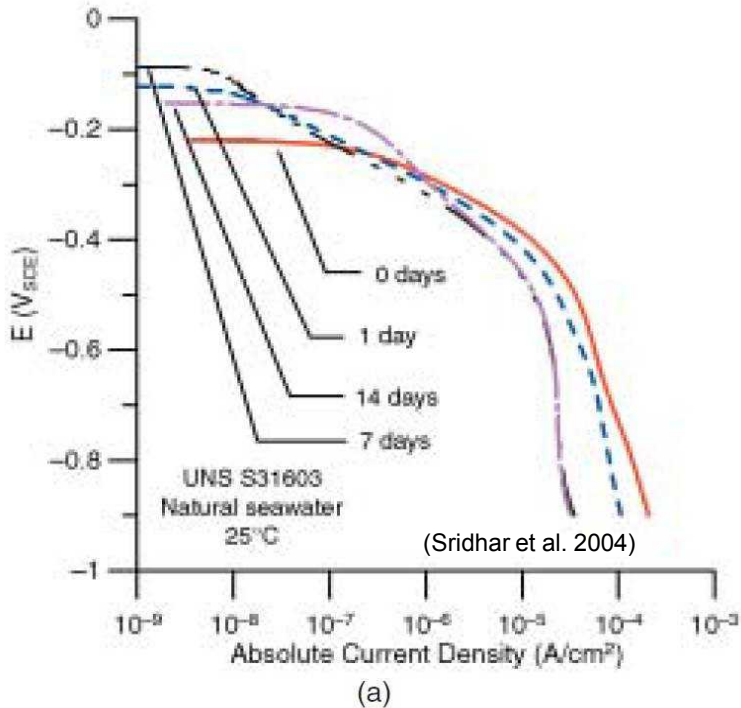
Assumption: Brine forms a continuous brine layer. This seems unlikely at low salt loads or low RH values. However:

- Experimental data suggest that the cathode can extend well beyond the perimeter of salt grains (*Schindelholz et al., 2013*), and cathodic reactions can cause salt redistribution on the metal surface
- Insoluble dust particles will increase brine film continuity via capillary effects.

Spent Fuel and Waste Science and Technology

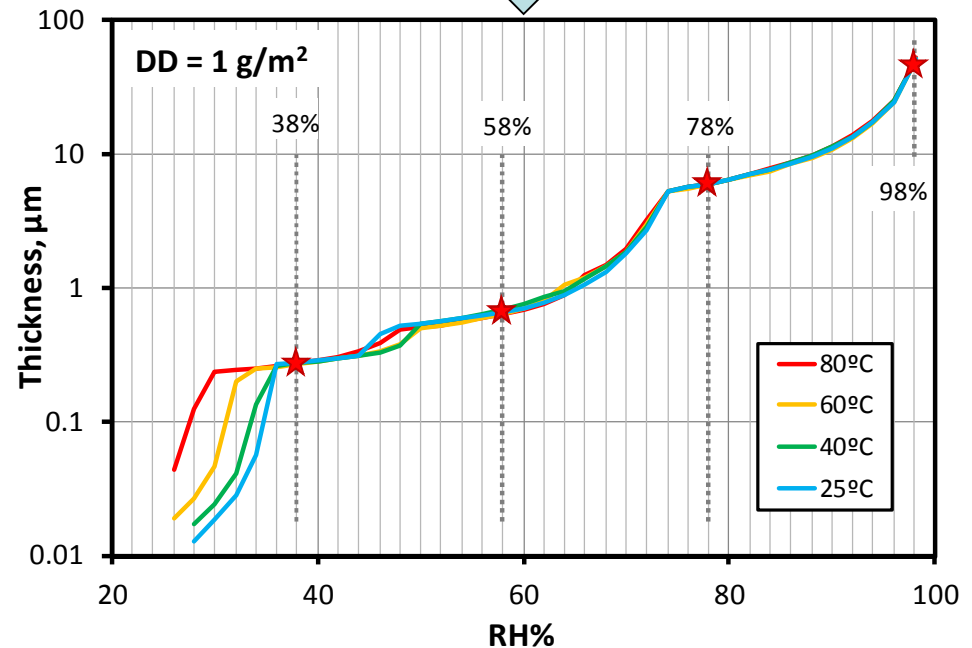
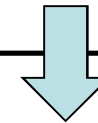
Other Needed Data: Cathodic Polarization Curves and electrochemical parameters for concentrated brines

Currently, limited available data:
Cathodic polarization curve for seawater at 25°C, 316 SS (Sridhar et al. 2004)



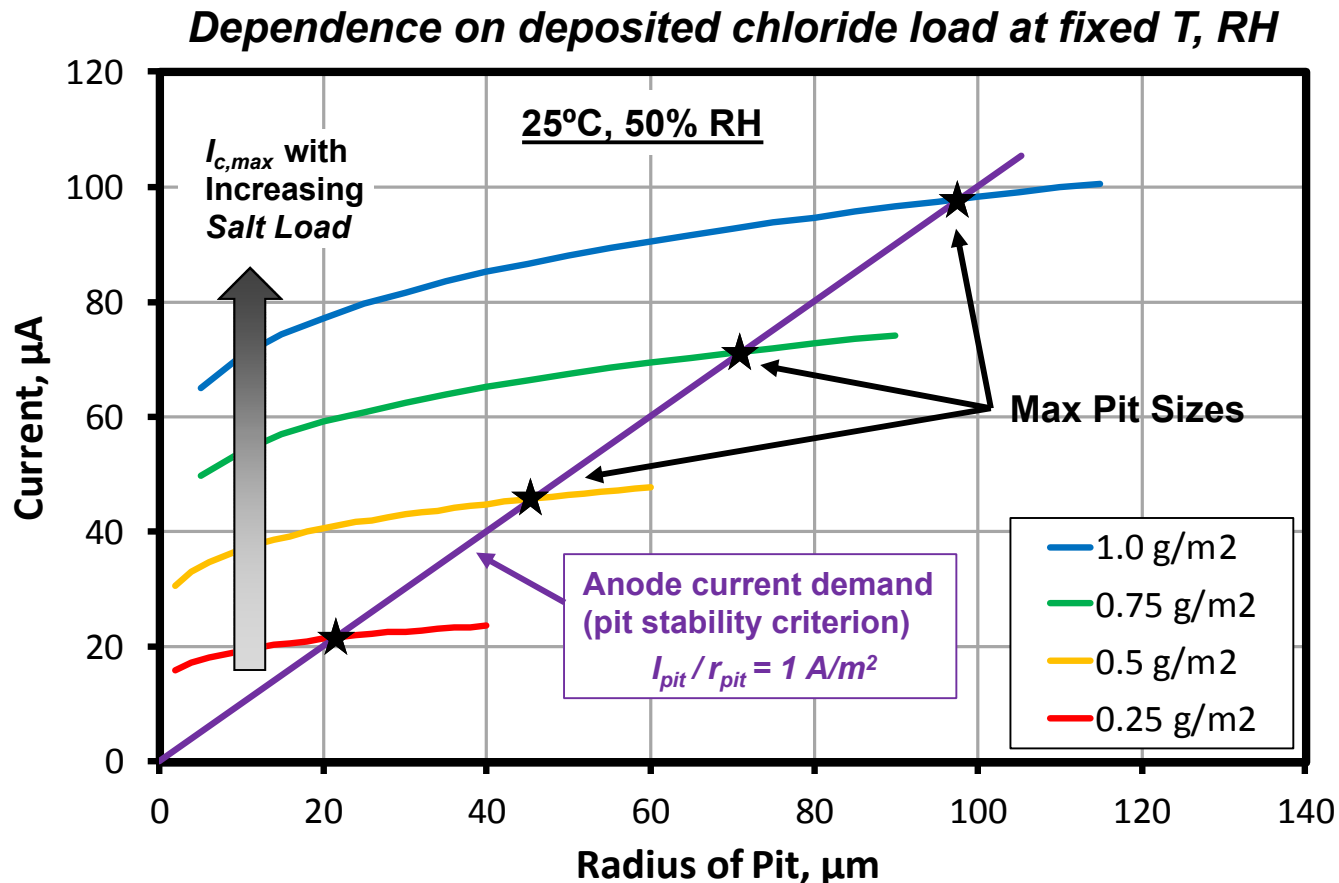
To characterize variability in cathode kinetics with brine composition, SNL is measuring polarization curves and other electrochemical parameters in four brines corresponding to:

- Unevaporated Seawater (98% RH)
- Evap. to 78% RH
- Evap. to 58% RH
- Evap. to 38% RH



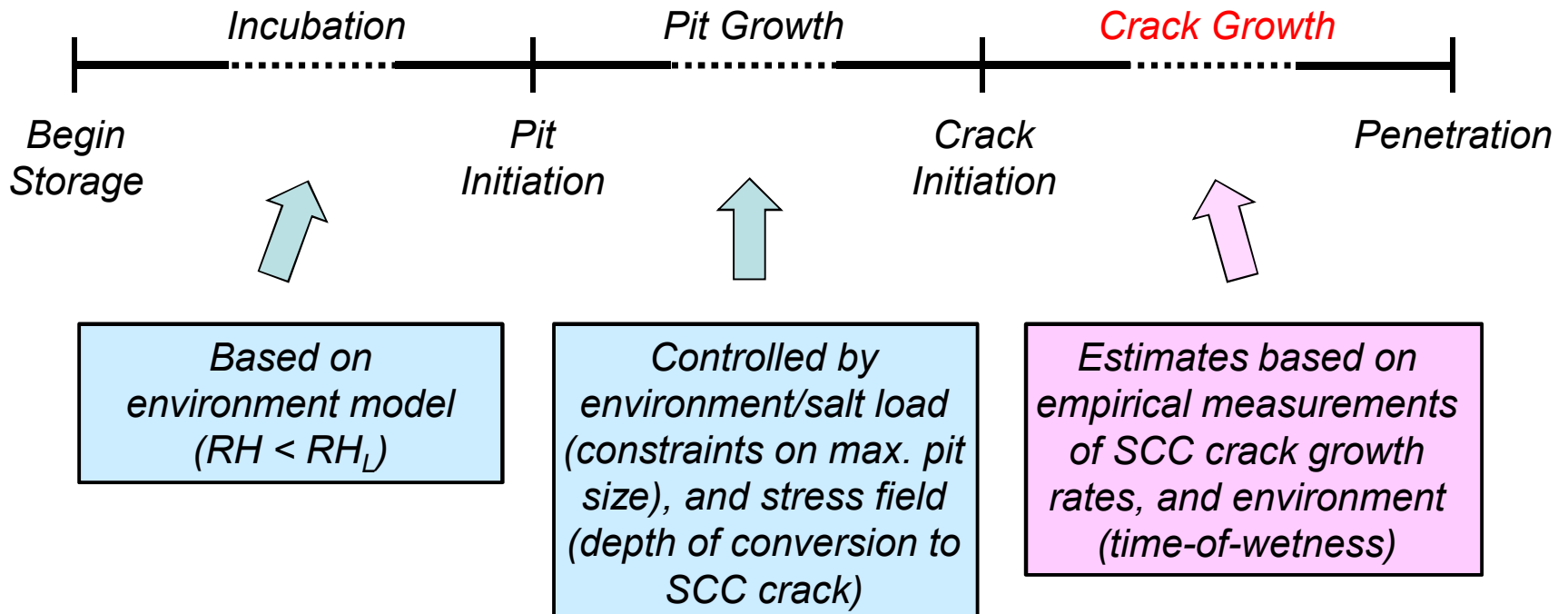
Determining Maximum Pit Size

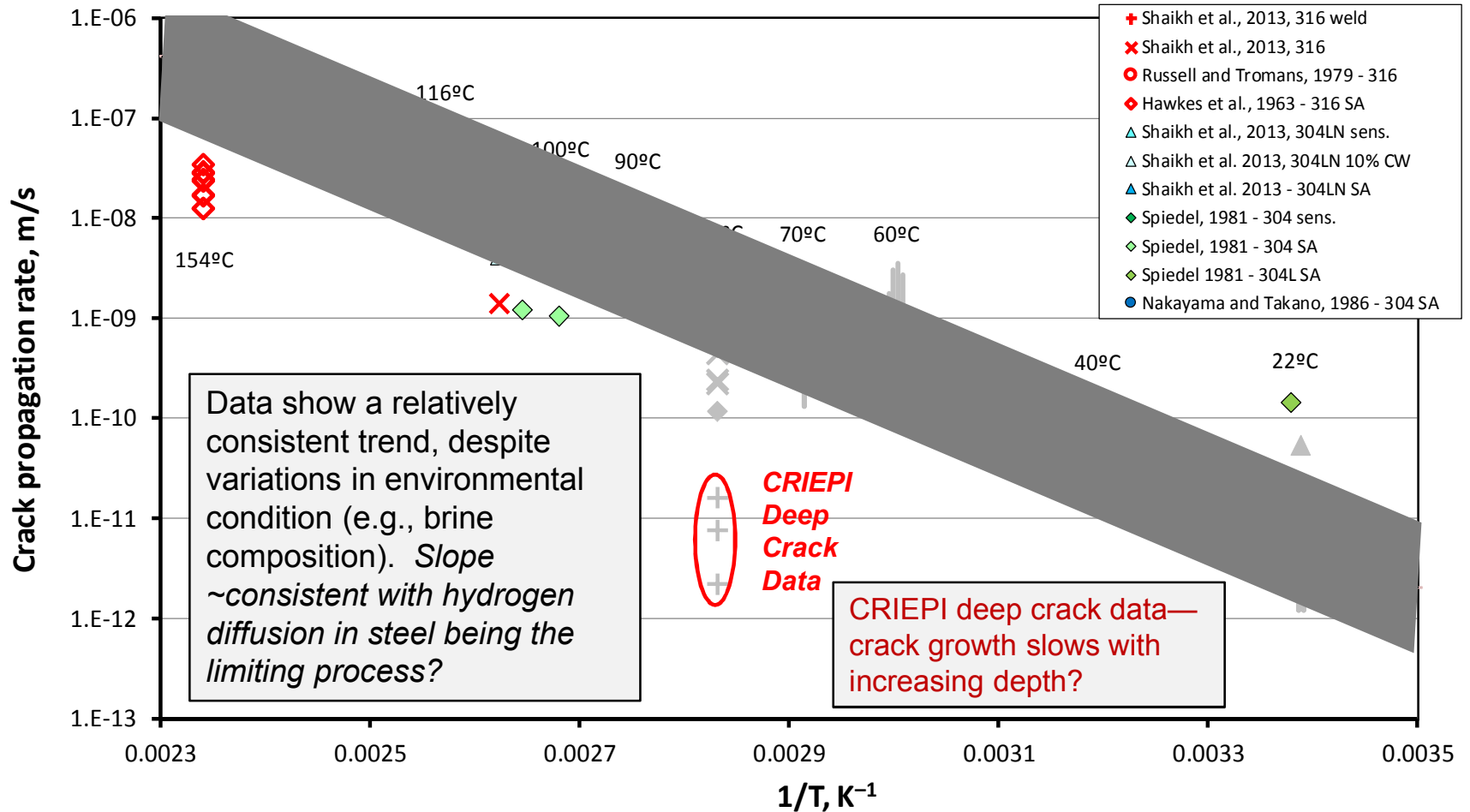
Maximum pit size is determined the intersection of the anode current demand and the available cathode current.



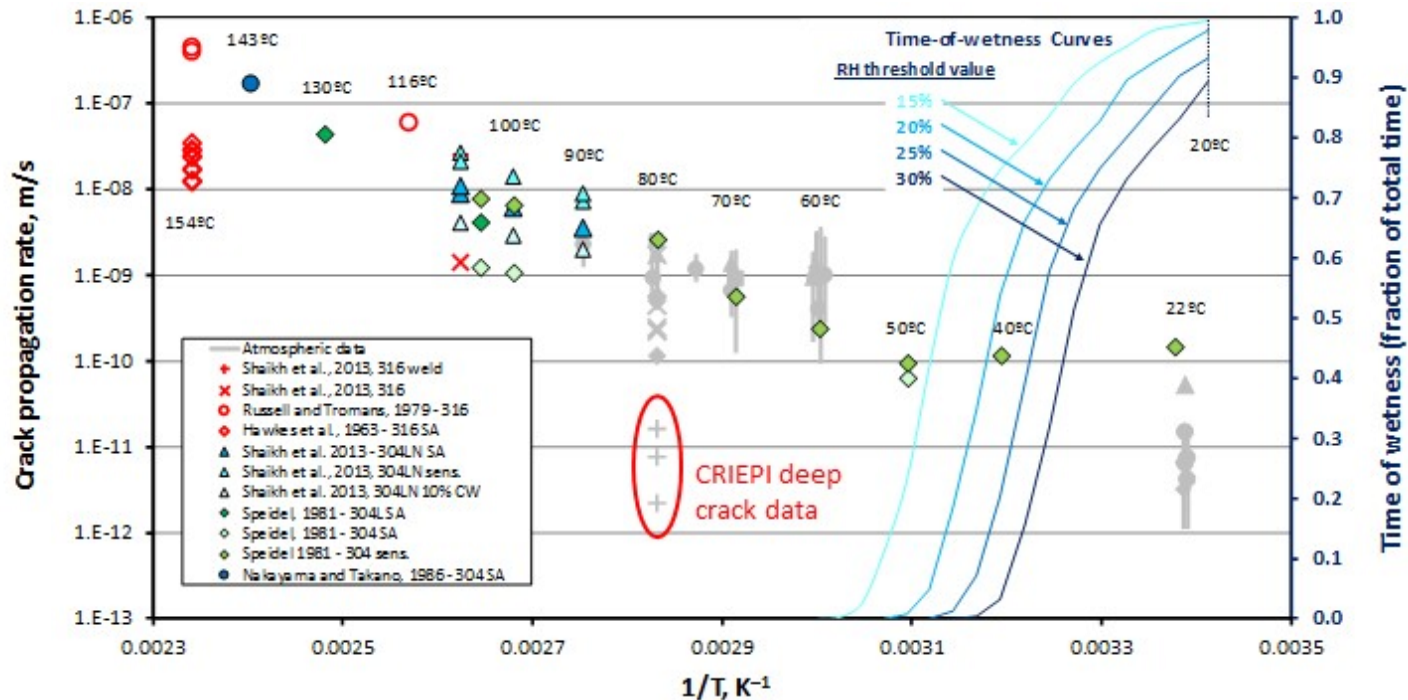
- **Long-term (2-year) pitting experiments, varying T, RH, salt load**
 - Test maximum pit size model
 - Evaluate salt redistribution in response to corrosion reactions
 - *Collaboration with Ohio State University*
- **Measurements of cathodic polarization curves on relevant brines**
 - *Collaboration with University of Virginia*
- **Effects of stress on pitting, and pit-to-crack transition**
 - *Collaboration with Colorado School of Mines*
 - *Collaboration with Ohio State University*

SCC Crack Growth





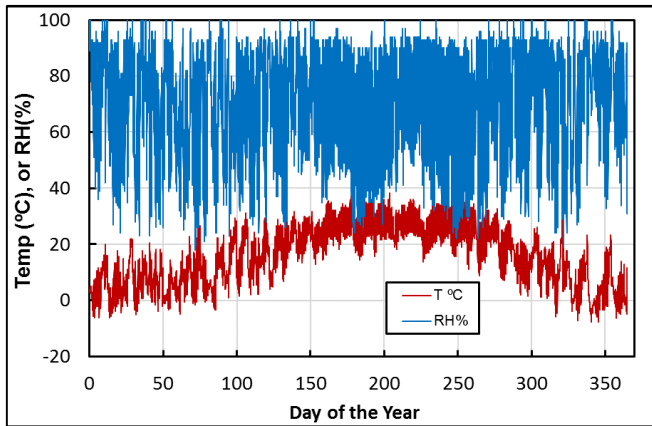
Time of wetness decreases with increasing temperature, limiting crack growth



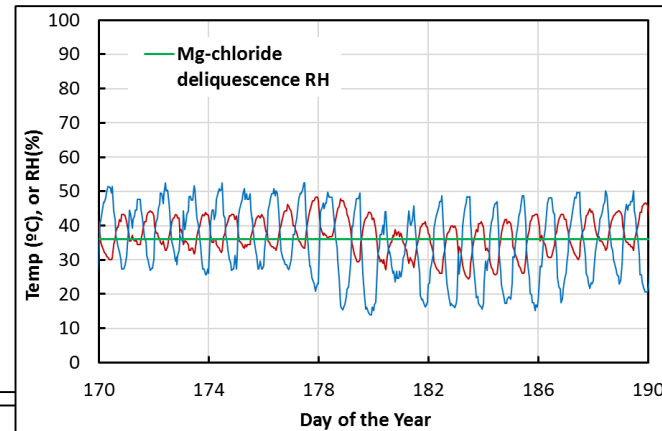
- Time-of-wetness concept based on removal of cathode during times of dry-out. Fairly well accepted for pitting, may not occur for stainless steel SCC:**
 - Some data (Andresen and Morra 2008) indicate that an external cathode is not necessary for stainless steel SCC.
 - Cracks are not as subject to dry-out (high capillarity, presence of highly deliquescent metal salts)

- **Effects of Brine Composition on CGR** (*Collaboration with North Carolina State University (CSM IRP)*)
- **Testing to evaluate time-of-wetness control on crack growth at SNL(?)**
 - *Use prototypical daily fluctuations in T and RH*

Weather near Arkansas Nuclear One



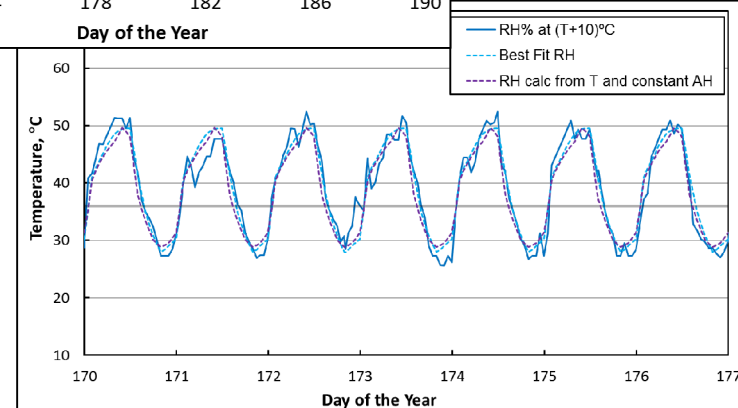
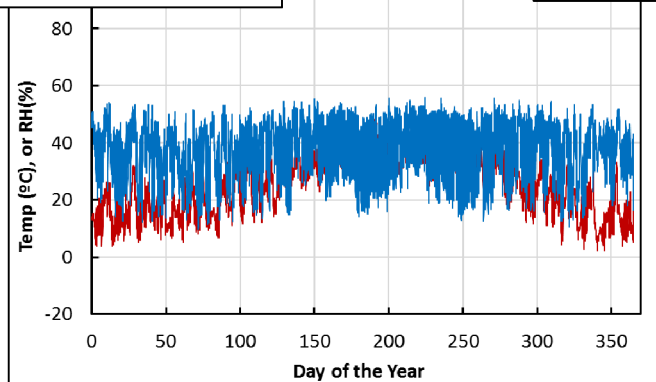
Focus on
region
crossing
DRH



Fit with simple
algorithm for lab
implementation



Add temperature
delta of 10°C



- **Initiation of corrosion controlled by deliquescence behavior of salts**
 - Assumption of sea-salts (MgCl_2 controls RH_D/RH_L) may be highly conservative
 - Elevated temperatures may be more protective for corrosion initiation and growth than we assumed (*especially in laboratory tests at accelerated conditions*).

- **Over time, cooling (increasing RH) and increasing salt loads result in:**
 - Thicker and more conductive brine films (potentially larger pits)
 - Larger pits → greater risk of SCC initiation (stochastic)

■ **Crack growth rates are difficult to predict**

- Probably a strong temperature dependence
- *May* be a cathodic limitation effect for atmospheric corrosion (thin brine films)
 - Crack growth *may* slow with increasing crack depth
 - Limited time-of-wetness with increasing temperature *may* limit penetration
 - Laboratory testing under realistic conditions very difficult

Spent Fuel and Waste Science and Technology

Backup slides

Knowledge Gaps:

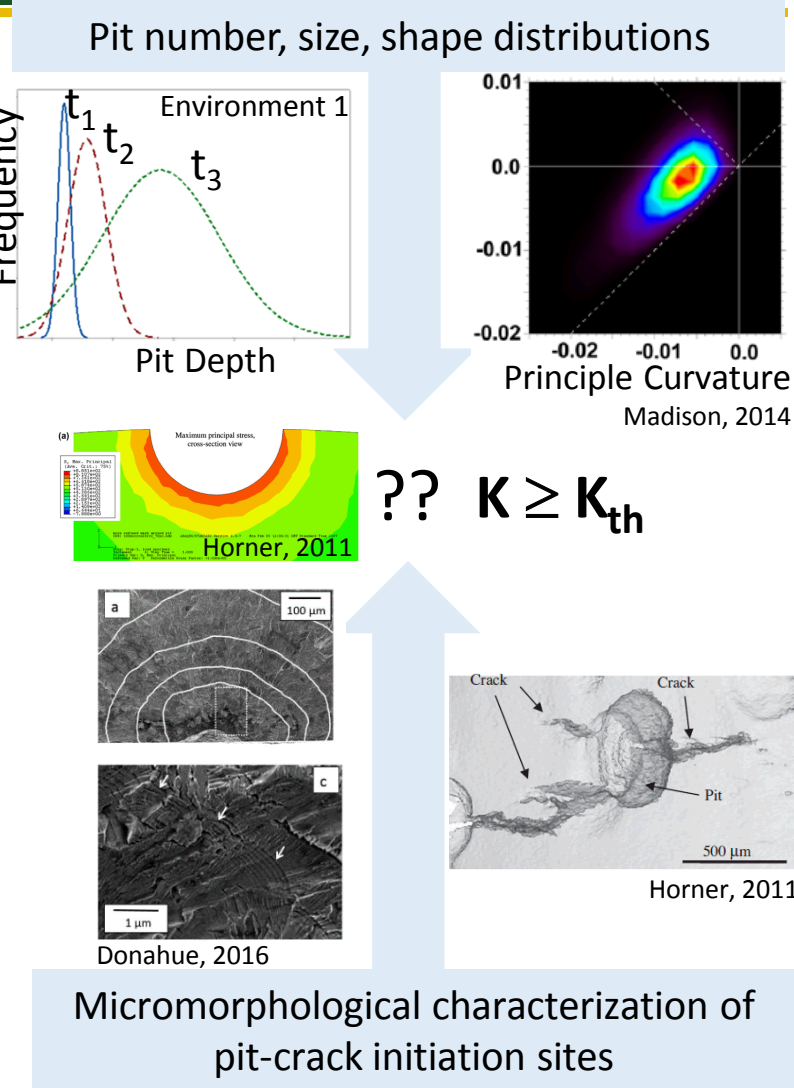
- Pitting kinetics, damage distributions (max pit size?) under ISFSI-relevant environmental conditions (T, RH, salt load)
- Pit-crack transition controlling factors

Goals:

- 1) Quantify relationship between environment and pitting damage distributions and rates
- 2) Identify hierarchical weakest links for pit corrosion feature to SCC crack transition

Approach:

- Parametric coupon-level pitting experiments in ISFSI-relevant environments
- Constant load marker band SCC tests in same environments to determine corrosion features that act as crack initiation sites



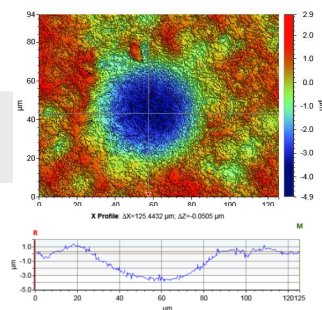
High-throughput Approach for Building Parametric Datasets



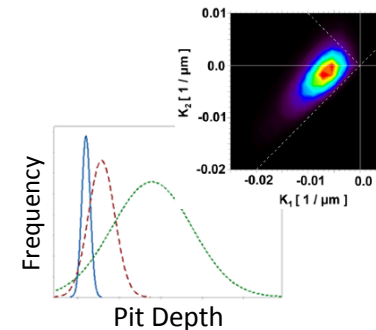
Inkjet printing for high-throughput salt loading

%RH	Temperature (°C)				
75	35				
70	35				
65	35				
60	35				
55	35	40			
50	35	40			
45	35	40	45		
40	35	40	45	50	55
35	35	40	45	50	
30	35	40	45	50	

ISFSI-Relevant Conditions



Optical profilometry and pit analysis (OSU)



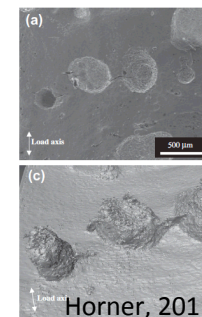
Pitting kinetics and shape distributions (SNL/OSU)

Approach:

- 304H coupon and tensile test bars loaded with artificial sea salt and exposed to fixed environmental conditions for up to 2 years
- Material details:
 - 304H, unsensitized and sensitized
 - Mirror, 120 grit “mill” finish
 - 10 and 300 ug/cm² seasalt



Serial Sectioning (SNL)



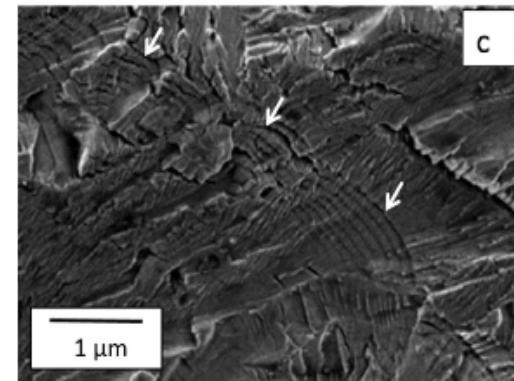
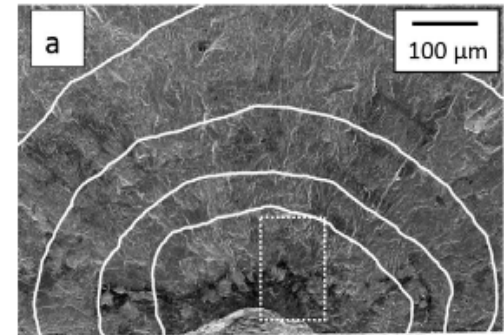
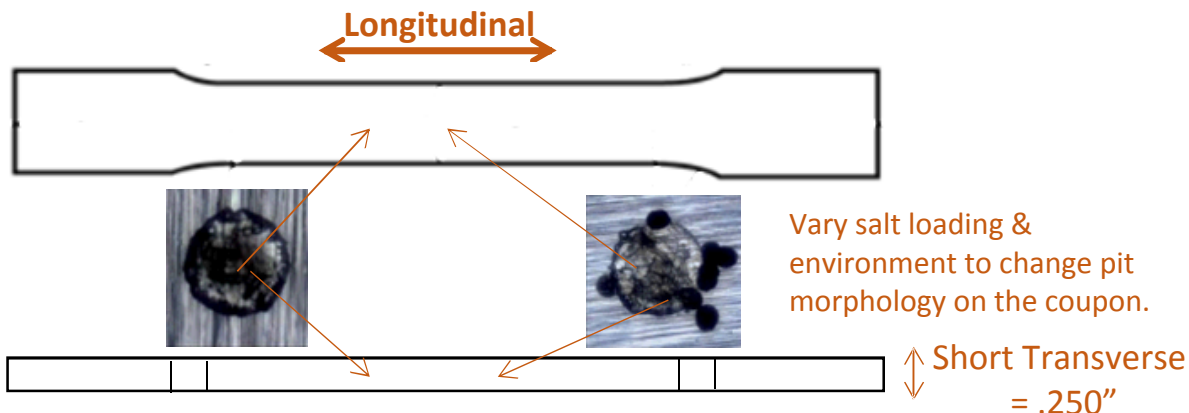
X-ray Microtomography (SNL)

Pit Micromorphology Characterization

Spent Fuel and Waste Science and Technology Pit to Crack Transition Study

Goal: Quantify the hierarchical weakest link for corrosion feature to SCC crack transition

- Variables:
 - Pit features (ex. narrow vs. wide)
 - Corrosion morphology (Single vs. Satellite Pits)
 - Material type
- Method: SCC testing
 - Gauge length of longitudinal tensile bars will be loaded with salt and corroded in a humidity controlled chamber.
 - Constant load with intermittent high R ripple fatigue loads during SCC tests to determine corrosion features that act as crack initiation sites.



J. R. Donahue and J. T. Burns, Effect of chloride concentration on the corrosion-fatigue crack behavior of an age-hardenable martensitic stainless steel, *International Journal of Fatigue* **91** (2016), 79-99.

Spent Fuel and Waste Science and Technology Plans – (2) SCC Testing

- *How does corrosion morphology affect crack initiation?*
- *Use same environmental conditions as coupon corrosion tests for SCC testing.*
 - *Pitting characteristics fully characterized for corrosion coupons/sacrificial tensile bars. This data will help explain cracking results.*



- *Load salt and corrode side of coupons (red)*
- *Remove from humidity chamber and print salt on face of coupon (green)*
 - *Extra salt on face will contribute electrolyte to the crack tip during propagation*

Sampling plan for corrosion coupons

Environment	Salt Load	1 wk	2 wk	1 mo.	6 mo.	12 mo.	18 mo.	24 mo.
35°C, 40%RH	300 µg/cm ²	X	X	X	X	X	X	X
35°C, 75%RH	10 µg/cm ²	X	X	X	X	X	X	X
35°C, 75%RH	300 µg/cm ²	X	X	X	X	X	X	X

**Matrix same as coupon tests, but with low-humidity / low-salt-load samples removed*

Knowledge Gaps:

- Relevance and accessible limits of existing deterministic damage models relative to canister conditions

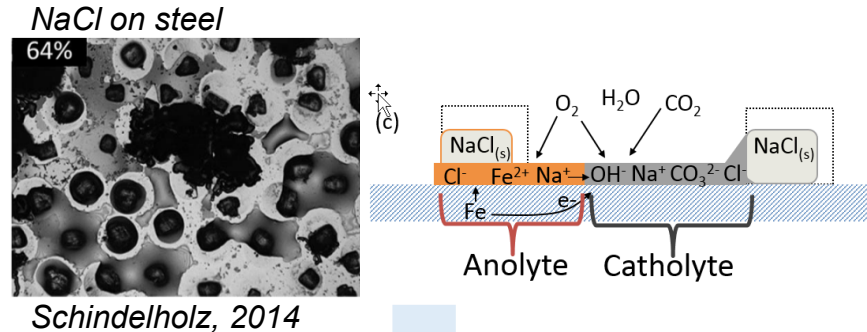
Goals:

- 1) Characterize electrolyte coverage and chemistry distribution during exposure in ISFSI-relevant environment
- 2) Quantify impact on electrochemical processes driving pitting and SCC

SNL: Eric Schindelholz, Charles Bryan, Chris Alexander

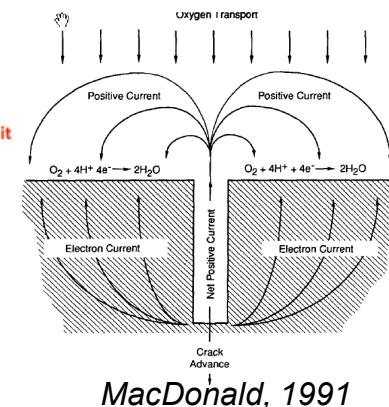
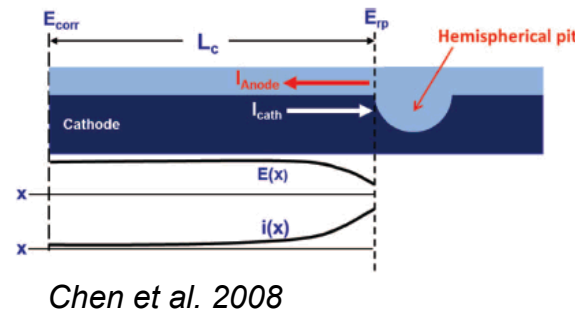
OSU/EFRC Jen Locke, Tim Weirich (PhD student)

CSM Zhenzhen Yu, Xin Wu



maximum pit size

crack growth rate (?)

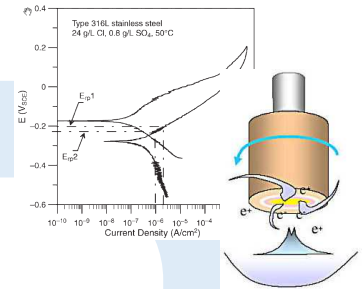
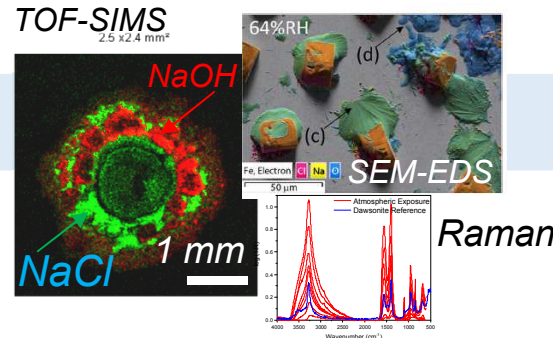


Spent Fuel and Waste Science and Technology

Impact of Corrosion on Surface Environment, Damage Distributions, and Rates: Coupon-Level Studies



%RH	Temperature (°C)				
75	35				
70	35				
65	35				
60	35				
55	35	40			
50	35	40			
45	35	40	45		
40	35	40	45		55
35	35	40	45	50	
30	35	40	45	50	



Inkjet printing for high-throughput salt loading

ISFSI-Relevant Conditions

Extent of electrolyte coverage and chemistry distribution

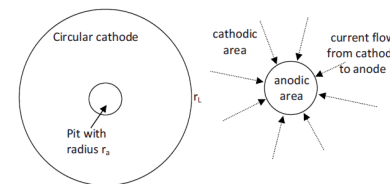
Cathodic and anodic kinetics in analog surface chemistries

Approach:

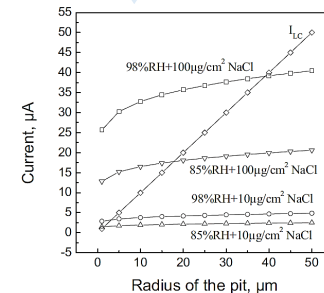
- Post-exposure surface analyses of coupons from pitting experiments:
- TOF-SIMS, MicroRaman/FTIR, Auger Spectroscopy
- Cathodic kinetics of 304 in analog surface chemistries (sea-salt brines, carbonate brines)
- Establish variance in max pit size model predictions due to evolving electrolyte, extend knowledge to CSM SCC electrochemical model

Max. cathode current, Brine conductivity, Brine layer thickness, Cathodic kinetics

$$\ln I_{c,max} = \frac{4\pi k W_L \Delta E_{max}}{I_{c,max}} + \ln \left[\frac{\pi e r_a^2 \int_{E_{corr}}^{E_{rp}} (I_c - I_p) dE}{\Delta E_{max}} \right]$$



Chen and Kelly, 2010



Knowledge Gap:

How material characteristics (microstructure, stress/strain) and environment (T, RH, salt load) impact electrochemical processes governing SCC

Goal:

Prediction of pitting and repassivation characteristics of 304 under varied static stress loads

Approach:

- Microelectrochemical mapping of CSM 4-point bend test specimens as a function of stress load
- Develop model to capture pitting characteristics as function of stress/strain with correlation to CSM 4-point bend atmospheric exposures

